Species-Specific Contribution of the Four C-Terminal Amino Acids of Influenza A Virus NS1 Protein to Virulence[▽]

Sébastien M. Soubies,[1,2] Christelle Volmer,[1,2] Guillaume Croville,[1,2] Josianne Loupias,[1,2] Brigitte Peralta,[1,2] Pierrette Costes,[1,2] Caroline Lacroux,[1,2] Jean-Luc Guérin,[1,2] and Romain Volmer[1,2]*

INRA, UMR 1225, Ecole Nationale Vétérinaire de Toulouse, F-31076 Toulouse, France,[1] and Université de Toulouse, ENVT, UMR 1225, F-31076 Toulouse, France[2]

Large-scale sequence analyses of influenza viruses revealed that nonstructural 1 (NS1) proteins from avian influenza viruses have a conserved C-terminal ESEV amino acid motif, while NS1 proteins from typical human influenza viruses have a C-terminal RSKV motif. To test the influence of the C-terminal domains of NS1 on the virulence of an avian influenza virus, we generated a wild-type H7N1 virus with an ESEV motif and a mutant virus with an NS1 protein containing a C-terminal RSKV motif by reverse genetics. We compared the phenotypes of these viruses *in vitro* in human, mouse, and duck cells as well as *in vivo* in mice and ducks. In human cells, the human C-terminal RSKV domain increased virus replication. In contrast, the avian C-terminal ESEV motif of NS1 increased virulence in mice. We linked this increase in pathogenicity in mice to an increase in virus replication and to a more severe lung inflammation associated with a higher level of production of type I interferons. Interestingly, the human C-terminal RSKV motif of NS1 increased viral replication in ducks. H7N1 virus with a C-terminal RSKV motif replicated to higher levels in ducks and induced higher levels of *Mx*, a type I interferon-stimulated gene. Thus, we identify the C-terminal domain of NS1 as a species-specific virulence domain.

Interspecies transmission of influenza viruses can lead to the introduction of new subtypes of influenza virus into the human population (31). The emergence of a new influenza virus that is able to spread efficiently between humans can cause a pandemic, as evidenced by the recent introduction of the swine-origin 2009 A/H1N1 virus to humans (10). The spread of avian influenza A viruses from birds to humans could also lead to the introduction of a new viral subtype with pandemic potential (22). Fortunately, the efficient replication of avian influenza A viruses in humans and interhuman transmission are generally limited and require further adaptations of the virus to humans. One determinant of host adaptation lies in the receptor binding specificity of hemagglutinin (HA) (52). In addition, several reports have underlined the role of amino acid 627 of the PB2 polymerase subunit in determining viral host range and virulence (15, 36, 44, 45). Large-scale sequence analyses of viruses isolated from different bird and mammalian species have been performed in order to identify previously unrecognized determinants of host adaptation and virulence (2, 32). Those studies have identified a 4-amino-acid motif in the C-terminal domain of NS1 that could represent a previously unnoticed host adaptation motif. Indeed, the vast majority of avian influenza viruses have an NS1 protein with a C-terminal ESEV domain, while typical human viruses have a conserved RSKV domain. The conservation of these species-specific motifs in the NS1 protein despite important sequence variability in the rest of the protein suggests that these four C-terminal amino acids are under strong selection pressure in their respective natural hosts (3, 5, 25).

NS1 is a multifunctional protein implicated in the regulation of viral gene expression and in the inhibition of the host antiviral response (12). In order to test the role of these newly identified NS1 domains, Jackson et al. previously introduced various C-terminal motifs into NS1 of the mouse-adapted human influenza virus A/WSN/33 strain by use of reverse genetics (24). Mice inoculated with a virus containing an avian C-terminal ESEV NS1 domain had high viral loads in the lungs and decreased survival compared to mice inoculated with a virus containing a C-terminal RSKV domain. These results showed that the C-terminal ESEV motif found in avian NS1 proteins increases virulence in mice when introduced into a human strain of influenza virus. Whether this finding also applies to avian influenza viruses remains unknown. Moreover, whether the C-terminal ESEV domain of NS1 increases replication in human cells remains unknown. Finally, how the C-terminal domains of NS1 modulate virulence in nonmammalian hosts, such as birds, is also unknown.

Here, we assessed the contribution of the C-terminal domains of NS1 to the pathogenicity of an avian influenza virus. By using reverse genetics, we generated H7N1 viruses containing an NS1 protein with a C-terminal avian ESEV domain or a C-terminal human RSKV domain. The replications of these viruses in human, mouse, and duck cell were compared. In addition, we assessed their pathogenicity in mice and ducks. Our results show that the C-terminal RSKV domain increases the replication of an avian influenza virus in human cells. To our surprise, we observed that the C-terminal RSKV domain increases replication in ducks. In contrast, the C-terminal ESEV domain increases virulence in mice. Thus, we identify

* Corresponding author. Mailing address: INRA, UMR 1225, Ecole Nationale Vétérinaire de Toulouse, F-31076 Toulouse, France. Phone: 33 5 61 19 32 33. Fax: 33 5 61 19 39 74. E-mail: rvolmer9@gmail.com.

▽ Published ahead of print on 21 April 2010.

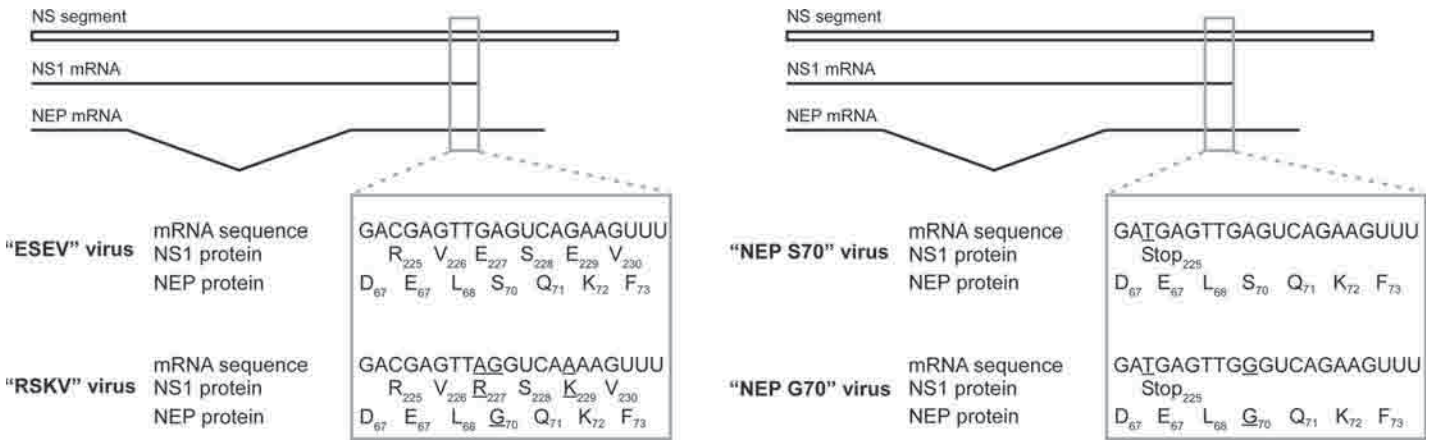

FIG. 1. NS segments of ESEV and RSKV and of NEPS70 and NEPG70. The NS segment of influenza A viruses encodes two proteins, named NS1 and NEP. The differences between the ESEV virus and the RSKV virus are underlined. The NEPS70 virus and the NEPG70 virus have a 224-amino-acid-long NS1 protein and differ from each other solely by the S70G mutation in NEP.

the C-terminal domain of NS1 as a species-specific virulence domain.

MATERIALS AND METHODS

Cells and reagents. Primary duck embryonic fibroblasts (DEF) were obtained from 10-day-old Pekin duck (*Anas platyrhynchos*) embryos. All cells, including human embryonic kidney (HEK) 293T cells, human A549 alveolar epithelial cells, mouse embryonic NIH 3T3 cells, and Madin-Darby canine kidney (MDCK) cells were grown in Dulbecco's modified Eagle's medium (DMEM) supplemented with penicillin (10^4 U/ml), streptomycin (10 mg/ml), and 10% fetal bovine serum at 37°C and 5% CO_2. The following antibodies were used: polyclonal rabbit serum directed against NS1 (kindly provided by D. Marc [INRA, Tours, France]), polyclonal rabbit anti-type A influenza virus nucleoprotein (NP) (kindly provided by G. Whittaker [Cornell University, Ithaca, NY]), mouse monoclonal antibody directed against type A influenza virus NP (Argene), and mouse monoclonal antibody directed against glyceraldehyde-3-phosphate dehydrogenase (GAPDH) (clone MAB 374; Chemicon).

Virus and reverse genetics. The low-pathogenicity avian influenza (LPAI) virus A/Turkey/Italy/977/1999 (H7N1) was a kind gift of I. Capua (Istituto Zooprofilattico Sperimentale Delle Venezie, Legnaro, Italy). The viral genome was extracted from allantoic fluid of embryonated chicken eggs infected with the LPAI A/Turkey/Italy/977/1999 (H7N1) virus (third egg passage) by using the QIAamp viral RNA minikit (Qiagen) according to the manufacturer's protocol. Each viral segment was cloned into vector pHW 2000, kindly provided by R. Webster (St. Jude Children's Research Hospital, Memphis, TN), as described previously (19, 20). In order to generate a mutant virus, site-directed mutagenesis was performed on the NS segment by using the QuikChange II kit (Stratagene) according to the manufacturer's protocol. The plasmid was then verified by sequencing.

HEK 293T cells were transfected with 0.3 μg of each of the eight pHW 2000 plasmids corresponding to the viral segments using the lipophilic transfection reagent LTX with Plus reagent (Invitrogen). To avoid multicycle replication in HEK 293T cells, no trypsin was added to the culture medium at this step. Three wells were transfected for each rescue and were respectively scraped at 24, 36, and 48 h posttransfection. Scraped cells and culture medium were then transferred onto DEF grown in Opti-MEM supplemented with 2 μg/ml L-(tosylamido-2-phenyl)ethyl chloromethyl ketone (TPCK) trypsin (Pierce). In order to produce viral stocks, viruses were further inoculated into 10-day-old embryonated chicken eggs. Titers of viral stocks were measured by standard plaque assay on MDCK cells. We verified the identity of amplified viruses by sequencing of amplicons of each viral gene segment using reverse transcription (RT)-PCR.

Infections and virus titration. All infections were performed with DMEM supplemented with 0.2% bovine serum albumin (BSA). TPCK trypsin (1 μg/ml) was added in the case of multiple-cycle growth analysis. The 50% tissue culture infectious dose ($TCID_{50}$) values were calculated by the Reed-Muench method with MDCK cells grown in 96 wells.

Mouse type I interferon (IFN) receptor blockade. Mouse 3T3 cells were infected at a multiplicity of infection (MOI) of 0.05 PFU per cell. After incubation for 1 h, the infection inoculum was replaced with fresh medium containing TPCK trypsin and 5 μg/ml of neutralizing anti-mouse alpha/beta interferon receptor 1 (IFNAR-1) antibodies (clone MAR1-5A3; Leinco Technologies) (8). Viral titers in the supernatant were measured by standard plaque assay on MDCK cells.

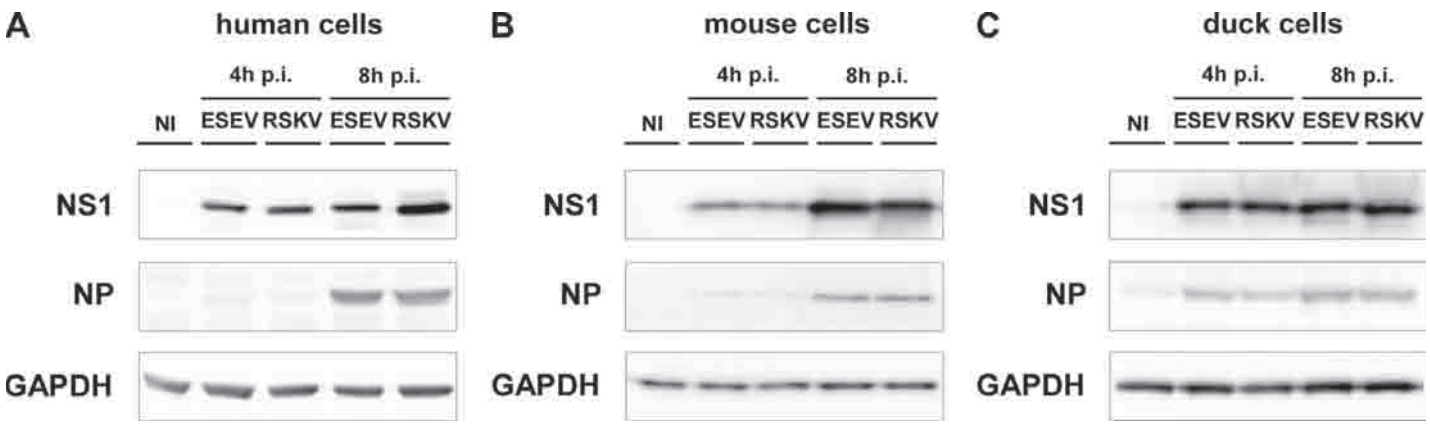

FIG. 2. Western blot analysis of human, mouse, and duck cells infected with ESEV and RSKV. Human A549 cells (A), mouse 3T3 cells (B), and primary duck fibroblasts (DEF) (C) were infected at an MOI of 3 with ESEV or RSKV. Cell lysates were collected at 4 and 8 h p.i. and analyzed by Western blotting against NS1 (top) and NP (middle). Western blotting with a GAPDH antibody (bottom) was used to show that equivalent amounts of protein were loaded. NI, noninfected cells used as controls.

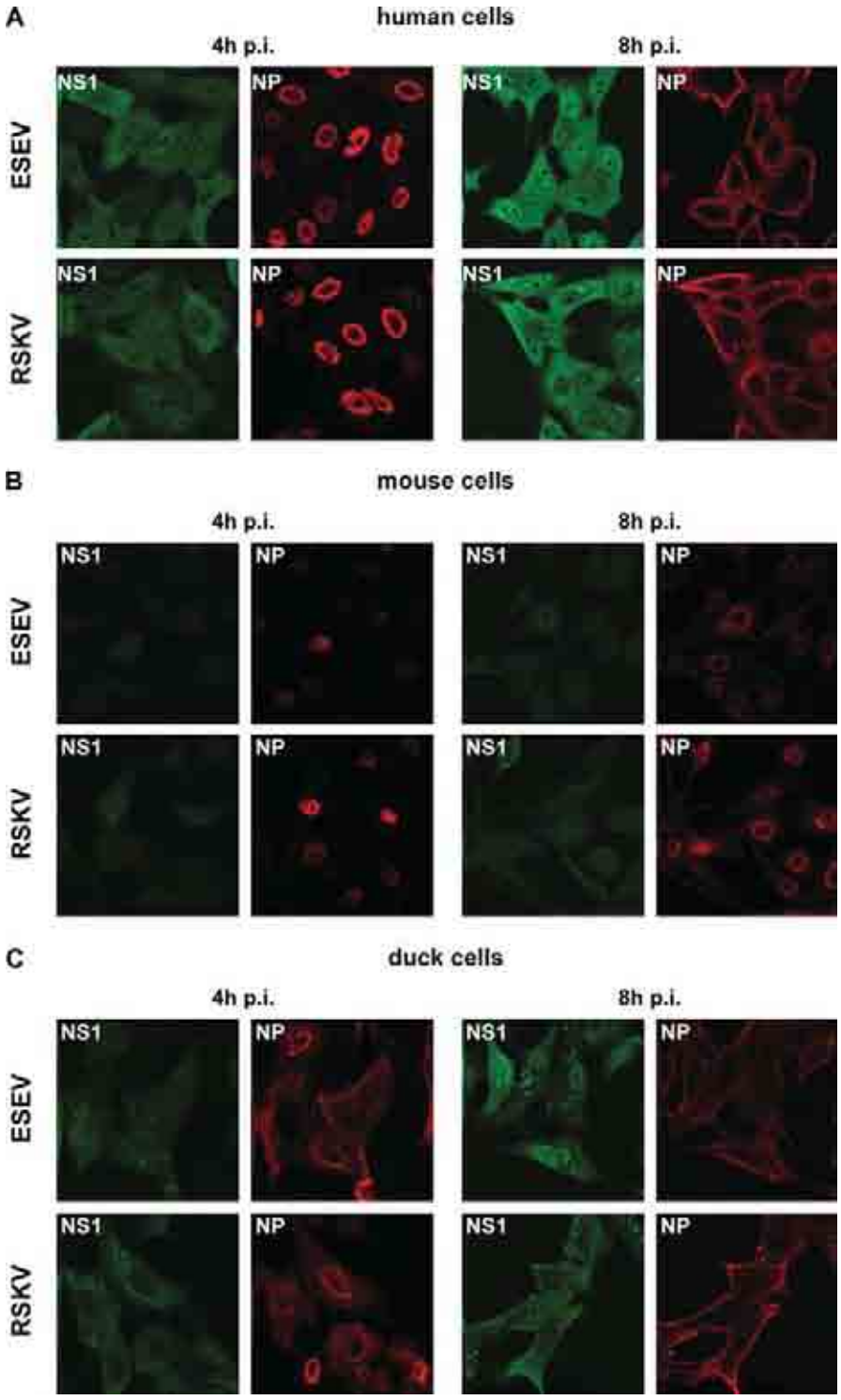

FIG. 3. Immunostaining of human, mouse, and duck cells infected with ESEV and RSKV. Human A549 cells (A), mouse 3T3 cells (B), and primary duck fibroblasts (DEF) (C) were infected at an MOI of 3 with ESEV or RSKV. Cells were fixed at 4 h p.i. (left) and 8 h p.i. (right). Immunostaining was performed with rabbit anti-NS1 and mouse anti-NP antibodies and revealed with appropriate secondary antibodies.

Western blots. Cells extracts and Western blot assays were performed as described previously (50). Nitrocellulose membranes were incubated with rabbit anti-NS1 polyclonal serum (1/1,0000 dilution), rabbit anti-NP polyclonal serum (1/5,000 dilution), and mouse anti-GAPDH (1/20,000 dilution). Horseradish peroxidase (HRP)-conjugated secondary antibodies were added; the chemiluminescent substrate Supersignal West Dura (Thermo scientific) was added, and the signal was imaged by using Bio-Rad Chemidoc XRS (Bio-Rad).

Immunostaining. Cells were fixed with 4% paraformaldehyde, permeabilized with phosphate-buffered saline (PBS)–0.5% Triton X-100, and incubated for 1 h in PBS–0.1% Triton X-100 and 2% BSA. Antibody incubation was performed overnight at 4°C by using polyclonal anti-NS1 rabbit serum (1/400 dilution) and monoclonal mouse anti-NP antibody (1/200 dilution). After washing, cells were incubated with rhodamine X-conjugated anti-mouse IgG (1/200 dilution; Jackson Immunoresearch) and fluorescein isothiocyanate (FITC)-conjugated anti-rabbit IgG (1/200 dilution; Jackson Immunoresearch) secondary antibodies. Coverslips were mounted in Vectashield (Vector Laboratories). FITC fluorescence and rhodamine X fluorescence were acquired sequentially with an Olympus confocal microscope.

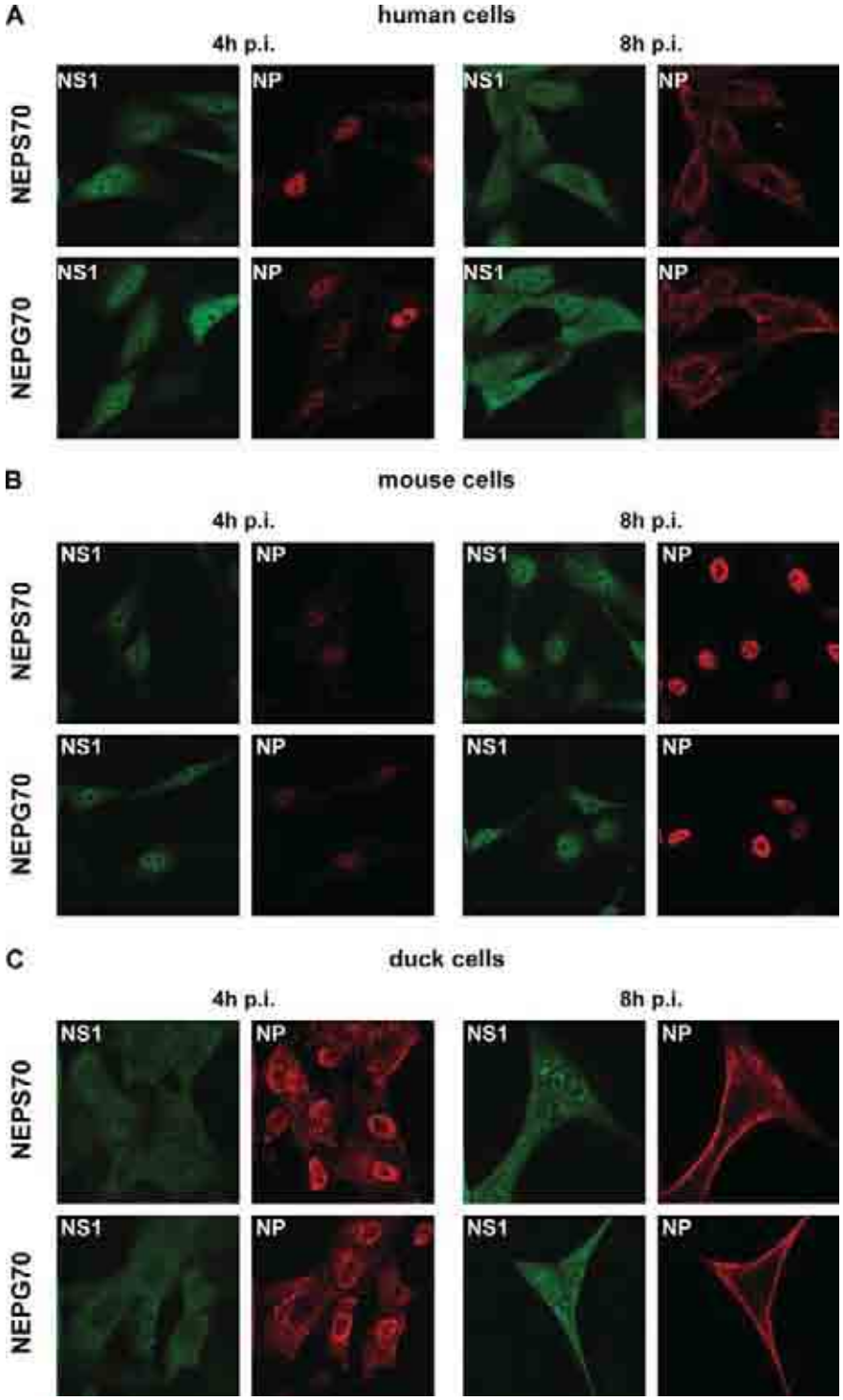

FIG. 4. Immunostaining of human, mouse, and duck cells infected with NEPS70 and NEPG70. Human A549 cells (A), mouse 3T3 cells (B), and primary duck fibroblasts (DEF) (C) were infected with ESEV or RSKV at an MOI of 3. Cells were fixed at 4 h p.i. (left) and 8 h p.i. (right). Immunostaining was performed with rabbit anti-NS1 and mouse anti-NP antibodies and revealed with appropriate secondary antibodies.

***In vivo* experiments.** All animals used in *in vivo* experiments were treated according to European Economic Community (EEC) recommendations for animal welfare and under the supervision of the local INRA Ethics Committee.

Two-week-old Pekin ducks (*Anas platyrhynchos domesticus*) were obtained from a commercial hatchery of controlled sanitary status (Couvoir de la Seigneurtière, Vieillevigne, France). We verified that animals had no anti-H7 antibodies prior to inoculation. Animals were inoculated with 10^7 PFU of virus diluted in PBS to reach a final volume of 500 μl, of which 250 μl was administered via the intrachoanal cleft route and 250 μl was administered via the oral route. Control animals were administered allantoic fluid from noninfected embryonated eggs that was diluted in PBS. Animals were maintained in HEPA-filtered isolation units. On days 1 and 6 postinfection (p.i.), six to seven animals in each group were euthanatized, and tissue samples were collected during necropsy. In a second experiment, 11 animals were infected as described above, and cloacal sampling was performed on days 2, 4, 6, 8, 10, 12, 14, and 18 p.i.

Four-week-old female BALB/c mice were obtained from Elevage Janvier (France). Animals were anesthetized with an intramuscular injection of ketamine and xylazine and inoculated intranasally with the indicated amount of virus

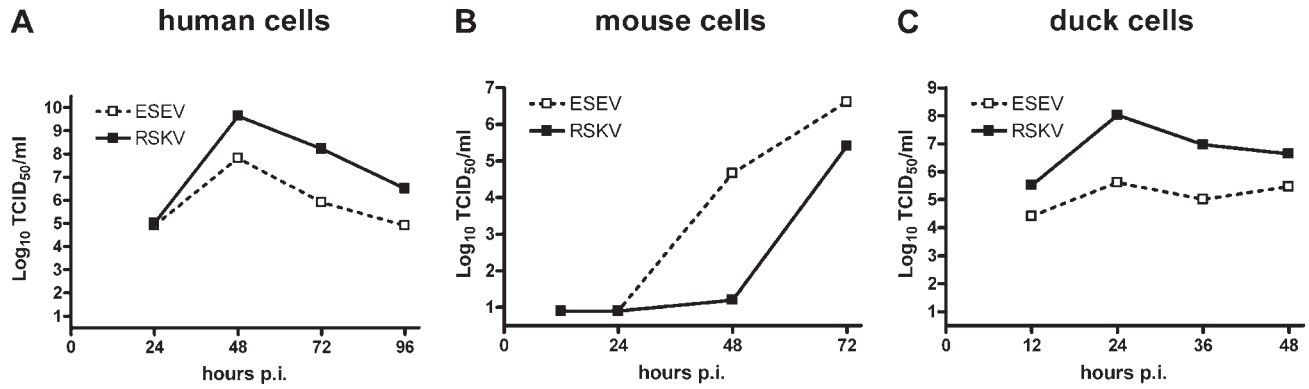

FIG. 5. Multiple-cycle growth analysis of human, mouse, and duck cells. (A and B) Human A549 cells (A) and mouse 3T3 cells (B) were infected at an MOI of 0.001. (C) Primary duck fibroblasts (DEF) were infected at an MOI of 0.0005 in the presence of TPCK trypsin to allow multiple-cycle virus growth. Supernatants were collected at the indicated times p.i., and viral titers were determined with MDCK cells. The results are representative of at least three independent experiments.

diluted in PBS to reach a final volume of 50 μl. Control animals were inoculated with allantoic fluid from noninfected embryonated eggs diluted in PBS. Body weight and clinical signs were monitored daily. Mice which had lost 25% of their initial body weight were euthanized according to the study protocol. On days 3 and 6 p.i., five animals under each condition were euthanized, and tissue samples were collected during necropsy.

Tissue samples were snap-frozen for virological analyses, snap-frozen in TRIzol reagent (Invitrogen) for RNA analyses, or kept in 10% neutral buffered formalin for histological analyses.

RNA extraction and quantitative PCR (qPCR). For *in vitro* experiments, RNA was extracted by use of the Nucleospin RNA II kit (Macherey Nagel).

RNA from organ samples conserved in TRIzol reagent (Invitrogen) was extracted according to the manufacturer's protocol. For each sample, 5 μg of RNA was further purified by use of the Nucleospin RNA II kit. Retrotranscription was performed by use of the SuperScript II reverse transcriptase kit (Invitrogen) and random primers (Invitrogen) according to the manufacturer's protocol. Quantitative PCR was performed with a final volume of 25 μl by using 5 μl of cDNA (diluted 10 times), each primer at 400 nM, and 12.5 μl of iTaq Sybr green supermix with ROX (Bio-Rad). All primers are available upon request.

Quantitative PCR was performed with Abi Prism 7000 SDS (Applied Biosystems) using the following program: initial denaturation (2 min at 95°C) followed by 40 cycles (15 s at 98°C and 1 min at 60°C) and a melting-curve analysis. To rule out genomic contamination, control PCR was performed in the absence of reverse transcriptase. For quantification, the ΔC_T was determined by comparing the cycle threshold numbers (C_T) required to reach a defined threshold value for the target gene versus a housekeeping gene (GAPDH). The relative amount of mRNA was then expressed as $2^{-\Delta CT}$.

In order to quantify viral RNA load, we used a QIAamp viral RNA minikit (Qiagen) followed by one-step RT-PCR (Quantitect; Qiagen) according to the manufacturer's protocol. Prior to RNA extraction, feces were weighed and diluted 1/10 in PBS, the ileum and colon were weighed, their mucosae were scraped away with a scalpel blade, and cloacal swabs were diluted in 500 μl PBS. Data were quantified by using standards consisting of 10-fold dilutions of a plasmid containing the viral sequence at a known concentration.

Histological analysis and immunohistochemistry. After 48 h of fixation in 10% neutral buffered formalin, tissues were routinely processed and embedded in paraffin. Sections were cut at 3 μm and stained with hematoxylin and eosin (H&E). Viral staining was performed with a mouse monoclonal antibody directed against NP (Argene) diluted 1/50 and incubated overnight at 4°C. A goat anti-mouse peroxidase polyclonal serum (Dako) was used as a secondary antibody. Diaminobenzidine (DAB) was used as the substrate chromogen, and slides were counterstained with hematoxylin.

A histopathological analysis was done by a veterinary pathologist who was blinded to the experimental conditions. In mice, the extent of inflammation and necrosis in the respiratory tract was graded as follows: 0 (no lesion), 1 (<10% of trachea, bronchi, and bronchioles affected and rare alveoli affected), 2 (<50% of trachea, bronchi, and bronchioles affected and alveolar areas affected), and 3 (>50% of trachea, bronchi, and bronchioles affected and alveolar areas affected). In ducks, the extent of inflammation in the ileum and the colon was graded as follows: 0 (no increase in cellularity in the *lamina propria*), 1 (scattered groups of inflammatory cells in the *lamina propria*), 2 (thickening of the *lamina propria* and separation of crypts by more than five strata of inflammatory cells), and 3 (diffuse and severe thickening of the *lamina propria* and separation of crypts by more than 10 strata of inflammatory cells). In ducks, the extent of necrosis in the ileum and the colon was graded as follows: 0 (normal mucosa), 1 (focal epithelial cell desquamation), 2 (more marked epithelial injury with eroded areas), and 3 (ulceration of epithelium). The histological score presented is the sum of the inflammatory and necrotic scores.

Reporter gene assays to measure human and duck type I IFN production. The titration of human type I IFN was performed by transfecting HEK 293T cells with a plasmid encoding firefly luciferase under the control of the interferon-stimulated response element (ISRE) enhancer (pISRE; Stratagene) and a plasmid containing the sequence of *Renilla* luciferase under the control of the herpes simplex virus TK promoter (TK-RLuc; Promega). At 16 h posttransfection, cells were stimulated with supernatants from infected cells (virus in the supernatant was inactivated by acid treatment at pH 2) or recombinant human IFN-α2a (HumanZyme) for 16 h. The activity of firefly luciferase was then measured with an Infinite 200 96 plate reader (Tecan) using the Dual-Glo luciferase assay system (Promega) and was normalized to the *Renilla* luciferase activity.

Titration of duck type I IFN was performed by transfecting DEF with a plasmid containing the sequence of firefly luciferase under the control of a chicken *Mx* promoter (Mx-FFLuc), kindly provided by P. Staeheli (Universität Freiburg, Freiburg, Germany) (38) and TK-RLuc, as previously described (42).

Sequence analysis of viruses in ducks and mice. Viral RNA was extracted from duck cloacal swabs or from mouse lung homogenates by using the QIAamp viral RNA minikit (Qiagen) according to the manufacturer's protocol. Retrotranscription and PCR were performed with NS-specific primers. PCR products were then cloned into vector pSC-B (Strataclone blunt PCR cloning kit; Stratagene). Four to thirteen clones of each virus were sequenced.

Data analysis. Data are presented as means ± standard errors of the means (SEM). For experiments analyzing the effect of type I IFN pretreatment on virus replication, statistical significance was assessed by using an unpaired, one-tailed Student's *t* test. For the other data, statistical significance was assessed by using an unpaired, two-tailed Student's *t* test.

RESULTS

Rescue of recombinant H7N1 viruses. We used the low-pathogenic avian influenza (LPAI) virus A/turkey/Italy/977/1999 (H7N1) strain to study the role of the recently identified conserved C-terminal domains of the NS1 protein (32). Plasmid-driven reverse genetics were used to recover wild-type virus that contains an NS1 protein with a typical avian ESEV C-terminal motif. We called this virus ESEV. In parallel, we mutated the NS segment to introduce the C-terminal RSKV domain into the NS1 protein (Fig. 1). The recovered mutant virus had an NS1 protein with a typical human C terminus and was designated RSKV. It should be noted that the E227R mutation in NS1 inevitably introduces a mutation in the amino

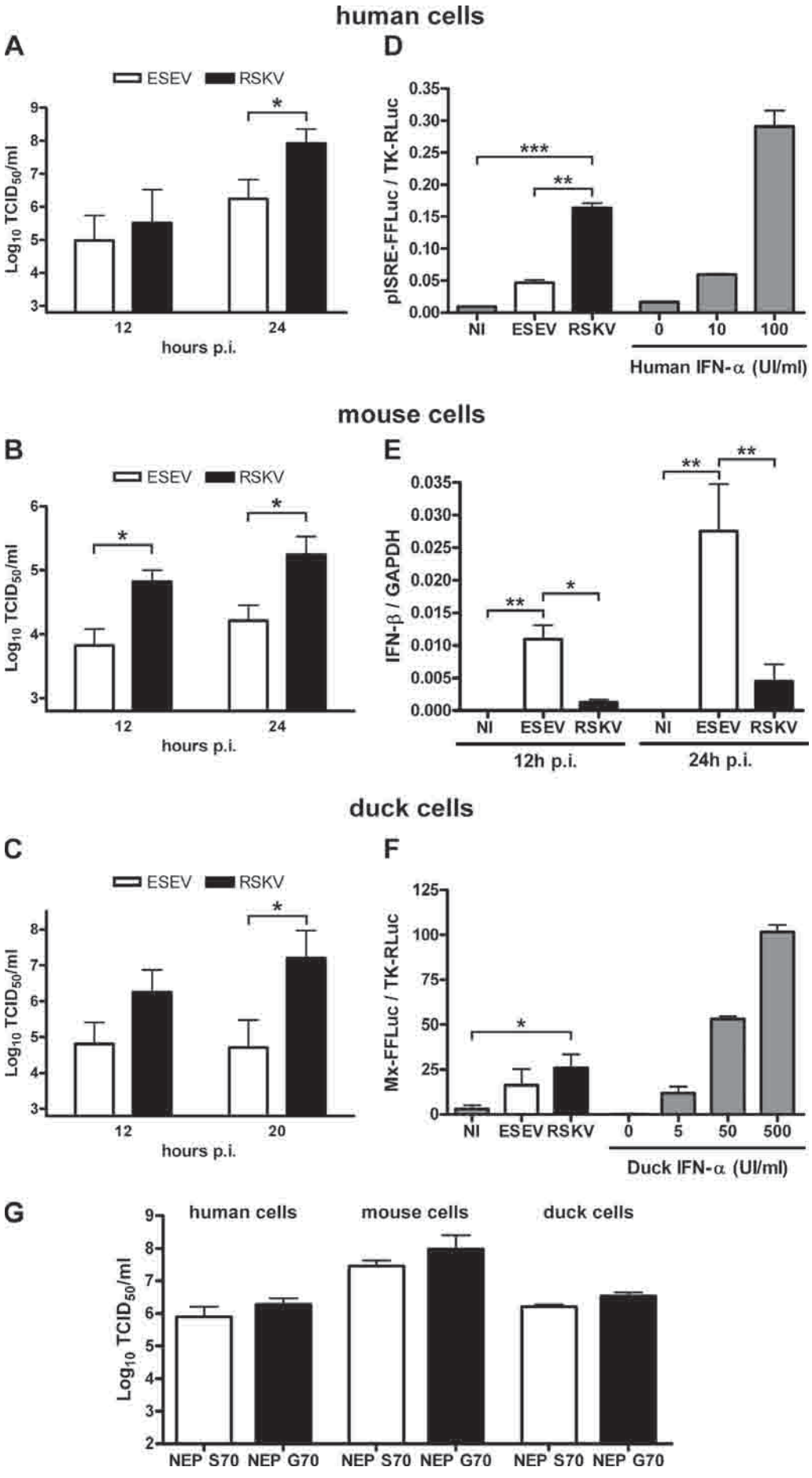
human cells
A
ESEV
RSKV
Log10 TCID50/ml
hours p.i.
12
24
D
pISRE-FFLuc / TK-RLuc
NI
ESEV
RSKV
Human IFN-α (UI/ml)
mouse cells
B
E
IFN-β / GAPDH
12h p.i.
24h p.i.
duck cells
C
F
Mx-FFLuc / TK-RLuc
Duck IFN-α (UI/ml)
G
human cells
mouse cells
duck cells
NEP S70
NEP G70

acid sequence of the nuclear export protein (NEP), which is encoded in a +1 reading frame from an alternatively spliced NS transcript. Thus, in conjunction with the E227R mutation in NS1, we also introduced an S70G mutation into NEP. Large-scale sequence analyses of influenza virus genomes have highlighted this coding constraint (2, 32). Indeed, a coselection of NS1 E227 and NEPS70 is apparent in avian influenza viruses, whereas a coselection of NS1 R227 and NEPG70 is apparent in human influenza viruses.

To test the impact of the S70G mutation on NEP, we used reverse genetics to rescue two other H7N1 viruses that differ only by the S70G mutation in NEP (Fig. 1). These viruses have a 224-amino-acid-long NS1 protein whose coding sequence is not affected by the S70G mutation in NEP. We called these viruses NEPS70 and NEPG70.

Analysis of NS1 and NP expression in human, mouse, and duck cells. As a first step toward the characterization of the ESEV and RSKV viruses, we analyzed the expression of NS1 and NP in human A549 alveolar epithelial cells, in mouse embryonic 3T3 fibroblasts, and in DEF infected at an MOI of 3 PFU per cell.

In all cell types tested, the levels of NP or NS1 expression analyzed by Western blotting at 4 h and 8 h p.i. did not differ significantly between ESEV and RSKV (Fig. 2). The NP and NS1 proteins were expressed at a lower level in human and mouse cells at 4 h p.i. than in duck cells. These results indicate that ESEV and RSKV are both able to infect human and mouse cells but with slower replication kinetics than those for duck cells. Importantly, the intracellular localizations of NP assessed by immunofluorescence analysis were also similar for both viruses. In human cells, NP was nuclear at 4 h p.i. and was found concentrated in the cytoplasm at 8 h p.i. (Fig. 3A). In mouse cells, NP was nuclear at 4 h p.i. and was also found in the cytoplasm at 8 h p.i. (Fig. 3B). In duck cells, NP was nuclear and cytoplasmic at 4 h p.i. and was concentrated below the cytoplasmic membrane at 8 h p.i. (Fig. 3C). These results suggest that the S70G mutation introduced into NEP does not impair the nuclear export of viral ribonucleoprotein complexes detected with the NP antibody. In human and mouse cells, the intracellular localizations of NS1 were similar for both viruses: NS1 localized mostly in the nucleus at 4 h p.i. and localized in the nucleus and cytoplasm at 8 h p.i. (Fig. 3A and B). Interestingly, the intracellular localizations of NS1 differed between the two viruses in duck cells. NS1 of ESEV localized mostly in the nucleus at 4 and 8 h p.i., whereas NS1 of RSKV appeared to be more cytoplasmic than nuclear (Fig. 3C). In addition, bright cytoplasmic foci of NS1 were detected in the cytoplasm of ESEV-infected duck cells at 4 h and 8 h p.i. These foci were reminiscent of previously described virus-induced cytoplasmic inclusions that remain of uncertain identity (34). Taken together, these results suggest that ESEV and RSKV do not differ in their abilities to infect human, mouse, and duck cells and that both viruses initiate replication with similar kinetics. However, the intracellular localizations of NS1 differ between ESEV and RSKV in duck cells.

Similar experiments were performed with the NEPS70 and the NEPG70 viruses. No difference in NS1 and NP immunofluorescence staining patterns was observed between these viruses, further suggesting that the S70G mutation does not significantly modify the functions of NEP in human, mouse, and duck cells (Fig. 4).

Multiple-cycle growth analysis of human, mouse, and duck cells. We next compared the growth properties of ESEV and RSKV in human, mouse, and duck cells infected at a low MOI. In human cells infected at an MOI of 0.001, RSKV replicated better than ESEV, reaching titers 60 times higher by 48 h p.i. (Fig. 5A). In contrast, ESEV virus replicated better than RSKV virus in mouse cells infected at an MOI of 0.001, reaching titers 10^3 times higher by 48 h p.i. (Fig. 5B). Finally, in duck cells infected at an MOI of 0.0005, RSKV replicated better than ESEV, reaching titers 10^2 times higher by 24 h p.i. (Fig. 5C). Altogether, these results indicate that the C-terminal domain of NS1 modulates viral growth in a host-specific way: in the context of an H7N1 avian influenza virus strain, the typical avian C-terminal ESEV domain enhances viral growth in mouse cells, whereas the typical human RSKV domain enhances viral growth in human and duck cells.

Analysis of single-cycle growth and type I interferon production in human, mouse, and duck cells. The level of replication during multiple-cycle growth results from the interplay between the intrinsic growth speed of the virus and its sensitivity to host-dependent antiviral effectors (11). Growth speed was analyzed by measuring viral titers during single-cycle growth. In parallel, we measured type I IFN production.

In human cells, RSKV reached significantly higher titers than ESEV during single-cycle growth (Fig. 6A). Titers obtained at 24 h p.i. were more than 40 times higher for RSKV than for ESEV. In order to measure type I IFN production, we used a biological assay that allows the measurement of any human type I IFN. The level of type I IFN at 24 h p.i. was significantly higher in the supernatants from RSKV-infected human cells than in supernatants from ESEV-infected cells, as

FIG. 6. Single-cycle growth analysis and type I IFN production in infected human, mouse, and duck cells. (A to C) Human A549 cells (A), mouse 3T3 cells (B), and primary duck fibroblasts (DEF) (C) were infected with ESEV or RSKV at an MOI of 3. Supernatants were collected at the indicated times p.i., and viral titers were determined with MDCK cells. (D) pISRE-Firefly luciferase activity (pISRE-FFLuc) normalized to TK *Renilla* luciferase activity (TK-Rluc) was measured in cells stimulated with supernatant from ESEV- or RSKV-infected human A549 cells (MOI of 3; supernatant collected 24 h p.i.) (left) or increasing concentrations of recombinant human IFN-α2a (right). (E) 3T3 cells were infected with ESEV or RSKV at an MOI of 3. At 12 and 24 h p.i., cells were lysed, RNAs were extracted, and IFN-β and GAPDH mRNAs were quantified by RT-qPCR. Levels of IFN-β mRNAs were normalized to GAPDH mRNA. (F) Mx-Firefly luciferase activity (Mx-FFLuc) normalized to TK *Renilla* luciferase activity (TK-Rluc) was measured in cells stimulated with supernatant from ESEV- or RSKV-infected DEF (MOI of 3; supernatant collected 20 h p.i.) (left) or increasing concentrations of recombinant duck IFN-α (right). (G) Human A549 cells, mouse 3T3 cells, and primary duck fibroblasts (DEF) were infected with NEPS70 or NEPG70 at an MOI of 3. Supernatants were collected at 24 h p.i., and viral titers were determined with MDCK cells. Results are expressed as means ± SEM of data from at least three independent experiments. *, $P < 0.05$; **, $P < 0.01$; ***, $P < 0.001$ (by unpaired *t* test).

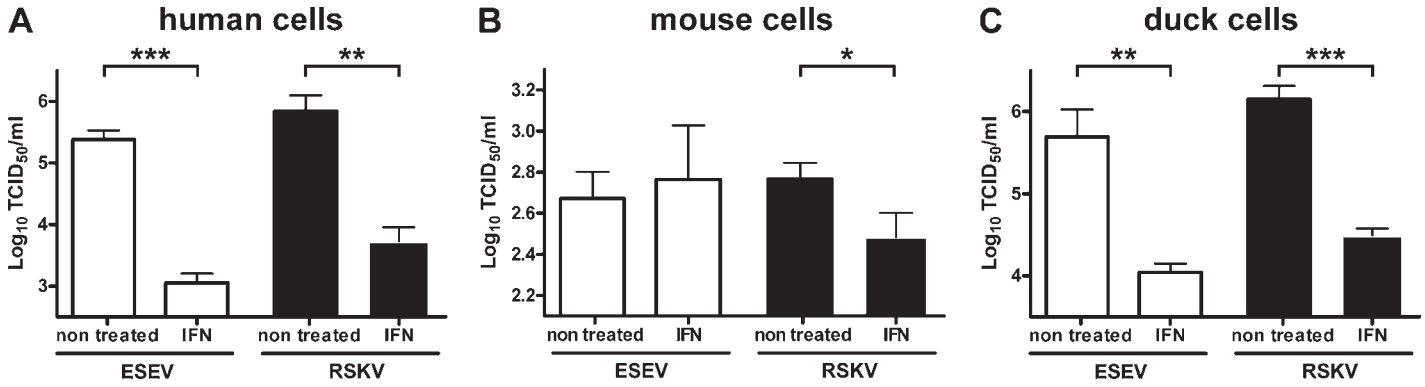

FIG. 7. Effect of IFN-α pretreatment on virus replication in human, mouse, and duck cells. Human A549 cells (A), primary duck fibroblasts (DEF) (B), and mouse 3T3 cells (C) were treated with 500 IU/ml of human, mouse, and duck recombinant IFN-α (rIFN-α), respectively, for 24 h and subsequently infected with the ESEV or RSKV virus (MOI of 0.1). Supernatants were collected at 24 h p.i., and viral titers were determined with MDCK cells. Results are expressed as means ± SEM of two experiments titrated in duplicate. *, $P < 0.05$; **, $P < 0.01$; ***, $P < 0.001$ (by one-tailed unpaired t test).

revealed by the higher signals obtained with this biological assay (Fig. 6D). Altogether, these results show that RSKV replicates to higher titers than ESEV during single-cycle growth in human cells and that this higher level of replication is associated with higher levels of type I IFN production.

In mouse cells, RSKV grew to significantly higher titers than ESEV during single-cycle growth (Fig. 6B), in sharp contrast with the results obtained during multiple-cycle growth experiments (Fig. 5B). This prompted us to analyze whether the reduced viral load observed for RSKV during multiple-cycle growth could be due to a higher level of type I IFN production. We therefore quantified IFN-β mRNA transcripts by RT-qPCR in mouse cells infected at an MOI of 3 at 12 h and 24 h p.i. Unexpectedly, IFN-β mRNA transcript levels were significantly elevated in ESEV-infected mouse cells compared to those in RSKV-infected cells (Fig. 6E). Thus, our results do not support the hypothesis that the reduced level of growth of RSKV during multiple-cycle growth in mouse cells could be due to a higher level of type I IFN induction.

In duck cells, RSKV reached significantly higher titers than ESEV during single-cycle growth (Fig. 6C). Titers obtained at 20 h p.i. were more than 200 times higher for RSKV than for ESEV. In order to measure type I IFN production, we used a biological assay that allows the measurement of any avian type I IFN (38). Supernatants from duck cells infected with the RSKV virus collected at 20 h p.i. exhibited an enhanced production of type I IFN compared to noninfected cells, as revealed by the higher signals obtained with this biological assay (Fig. 6F). However, no significant differences in type I IFN production were observed between ESEV- and RSKV-infected duck cells. Altogether, these results show that RSKV replicates more efficiently than ESEV during single-cycle growth in duck cells and that this higher level of replication is associated with a modest increase in the levels of type I IFN produced.

To assess whether the S70G mutation in NEP contributes to the differences in growth speed, we compared the single-cycle growth properties of the NEPS70 and NEPG70 viruses. The NEPS70 virus and the NEPG70 virus reached similar titers at 24 h p.i. in human, mouse, and duck cells (Fig. 6G). This result further suggests that the S70G mutation does not significantly modify the functions of NEP in human, mouse, and duck cells.

Impact of type I IFN pretreatment on virus replication in human, mouse, and duck cells. ESEV and RSKV could also differ in their sensitivities to type I IFN-induced antiviral effectors. We therefore evaluated virus growth in cells pretreated with type I IFN. Cells were pretreated for 24 h with 500 IU/ml of recombinant type I IFN and subsequently infected at an MOI of 0.1. In human and duck cells, type I IFN pretreatment led to a significant decrease in both ESEV and RSKV titers at 24 h p.i. (Fig. 7A and B). In mouse cells, type I IFN pretreatment also significantly inhibited RSKV replication (Fig. 7C). In contrast, ESEV replication was not inhibited, suggesting that ESEV was less sensitive to type I IFN pretreatment than RSKV in mouse cells (Fig. 7C). To further test how type I IFN sensitivity modulates viral growth in mouse cells, we compared the growth properties of ESEV and RSKV in mouse cells infected at an MOI of 0.05 and treated or not with saturating amounts of a neutralizing antibody against the murine type I IFN receptor IFNAR1. In untreated mouse cells, ESEV reached higher titers than RSKV. In contrast, in mouse cells treated with IFNAR1-neutralizing antibodies, RSKV reached higher titers than ESEV (Table 1). Altogether, these results suggest that in type IFN-competent mouse cells, ESEV reaches higher titers than RSKV during multiple-cycle growth because it is less sensitive to type I IFN than RSKV.

TABLE 1. Replication of ESEV and RSKV in mouse cells treated or not with neutralizing antibodies to mouse type I IFN receptor

Neutralizing antibody to mouse type I IFN receptor	Virus titer at 48 h p.i. (PFU/ml)[a]	
	−	+
ESEV	3.3×10^2	1.0×10^3
RSKV	1.5×10^2	6.5×10^3

[a] Mouse 3T3 cells were infected at an MOI of 0.05 in the presence of TPCK trypsin to allow multiple-cycle virus growth and treated with saturating amounts of a neutralizing antibody against murine IFNAR1 or left untreated. Results are representative of two independent experiments and are expressed as the means of duplicate titrations.

Impact of the ESEV and RSKV domains of NS1 on viral growth and pathogenicity in mice. We next evaluated the pathogenicity of ESEV and RSKV *in vivo*. We infected BALB/c mice intranasally with serial dilutions of ESEV and RSKV. Both viruses were rapidly lethal when inoculated at 10^7 PFU per mouse (Fig. 8A). However, ESEV appeared to be more virulent than RSKV at lower doses, causing a higher mortality rate when used at 10^6 PFU (Fig. 8A) and significantly more weight loss when used at 10^5 PFU (Fig. 8B). Histopathological analysis of the respiratory tract confirmed that ESEV was more pathogenic than RSKV (Fig. 8C and E). ESEV-infected mice had severe tracheobronchitis and bronchioloalveolitis, characterized by large areas of sloughed necrotic epithelial cells and extensive infiltrates of neutrophils and mononuclear cells. In ESEV-infected mice, alveolar spaces were filled with neutrophils, macrophages, cellular debris, and edema fluid. Pulmonary lesions in RSKV-infected mice were less severe and restricted to tracheobronchial and peribronchiolar areas. Immunohistochemical analysis revealed that the localization of NP-positive cells did not differ between ESEV- and RSKV-infected mice at day 6 p.i. (Fig. 8D). Viral antigen was located principally in the tracheal, bronchial, and bronchiolar epithelial cells. NP staining was also present in sloughed epithelial cells, in macrophages, and in a few small cuboidal cells lining alveoli that were reminiscent of type II pneumocytes. In order to test whether this increase in pathogenicity was due to a higher level of replication of ESEV, we measured viral titers in lungs of mice infected with 10^5 PFU. Viral titers were higher in ESEV-infected mice than in RSKV-infected mice at day 3 p.i. (Fig. 8F). At day 6 p.i., viral titers decreased in ESEV-infected mice, reaching levels similar to those found for RSKV-infected mice. Thus, viral pathogenicity, assessed by the extent of weight loss and the histological score, was not directly correlated with viral load. Instead, we could correlate pathogenicity to the level of type I IFN transcripts in the lungs of infected mice. ESEV induced significantly higher levels of IFN-β and IFN-α mRNA transcripts than RSKV at days 3 and 6 p.i. (Fig. 8G). Importantly, viral sequence analysis performed on three mice per group at day 6 p.i. revealed that no virus had acquired mutations affecting the coding sequence of the C-terminal domain of NS1 (Table 2). Together, our results show that the higher pathogenicity of ESEV in mice is associated with an increase in virus replication at day 3 p.i. and correlates with an increase in lung inflammation and a higher level of type I IFN induction.

Impact of the ESEV and RSKV domains of NS1 on viral growth and pathogenicity in ducks. We infected Pekin ducks via the oral and intrachoanal routes with 10^7 PFU of ESEV or RSKV. As expected for LPAI viruses, ducks did not exhibit any clinical signs over the whole duration of the experiment. However, histopathological analysis performed on days 1 and 6 p.i. revealed a mild to moderate inflammation of the ileum (Fig. 9A) and the colon (data not shown) of ESEV- and RSKV-infected ducks. Inflammatory infiltrates in the *lamina propria* were variably composed of both heterophils and mononuclear cells or solely of mononuclear cells. A mild necrosis of the ileal epithelium without any villus atrophy was observed for infected animals. Histological scores were low for infected animals yet significantly different from those of the ileum of noninfected animals (Fig. 9C). No significant differences were observed between histological scores of ESEV- and RSKV-infected ducks. Immunohistochemically, viral antigen was detected in differentiated epithelial cells of the ileum and the colon. No infected cells were detected in the trachea, indicating that ESEV and RSKV have a predominant intestinal tropism. In the intestine, ESEV-infected ducks had only a few NP-positive cells per cut at day 6 p.i., and most of them were found in the ileum (Fig. 9B). In contrast, RSKV-infected ducks had a higher number of NP-positive cells per cut at day 6 p.i., and the intensity of NP staining also appeared stronger.

The level of fecal excretion was quantified by measuring the amount of infectious viral particles and viral RNA copies per gram of feces (Fig. 9D and E). ESEV was excreted at higher levels than RSKV in the feces at day 1 p.i. In contrast, RSKV was excreted at higher levels than ESEV at day 6 p.i., but the difference did not reach statistical significance. We next analyzed viral load in the ileal and colonic mucosae by RT-qPCR. At day 1 p.i., no viral RNA was detected in the ileal and colonic mucosae of ESEV- or RSKV-infected ducks (data not shown). At day 6 p.i., viral RNA levels were significantly higher in the ileal mucosa of RSKV-infected ducks than in that of ESEV-infected ducks (Fig. 9F). Viral RNA levels were also higher in the colonic mucosa at day 6 p.i., but the difference did not reach statistical significance (Fig. 9F).

Next, we evaluated whether ESEV and RSKV induced different levels of type I IFN *in vivo*. However, the sequence of duck IFN-β is unknown, and we could not detect any upregulation of duck IFN-α transcription in the ileum and the colon of infected ducks by RT-qPCR (data not shown). We therefore measured tissue levels of type I IFN indirectly by quantifying *Mx* transcription. *Mx* is an interferon-stimulated gene and a good indicator of the level of type I IFN produced *in situ* (21, 40). RSKV induced significantly higher levels of *Mx* transcripts than ESEV in the ileum (Fig. 9G) and in the colon (data not shown) at days 1 and 6 p.i., likely reflecting a higher level of type I IFN production.

Finally, in a second experiment, we evaluated the duration of virus fecal excretion by detecting viral nucleic acids from cloacal swabs by RT-qPCR. Eleven ducks per group were monitored for 18 days p.i., and cloacal swabs were taken every 2 days. On day 4 and day 6 p.i., all ESEV- and RSKV-inoculated animals excreted virus (Fig. 9H). However, the number of animals excreting virus decreased rapidly from day 6 p.i. in the RSKV-infected group, whereas all ESEV-infected ducks still excreted virus until day 10 p.i. After day 10 p.i., the number of excreting animals also decreased in the ESEV-infected group. At day 18 p.i., cloacal swabs from RSKV-inoculated animals were all negative, and only one animal remained positive for virus in the ESEV-inoculated group. Altogether, the mean duration of fecal excretion was 12.6 ± 0.9 days (mean ± SEM) for ESEV versus 10.9 ± 1.0 days for RSKV. Thus, ESEV appeared to be excreted longer than RSKV. Importantly, viral sequence analysis of three positive cloacal swabs taken from each group on day 14 p.i. revealed that no virus had acquired mutations affecting the coding sequence of the C-terminal domain of NS1 (Table 2).

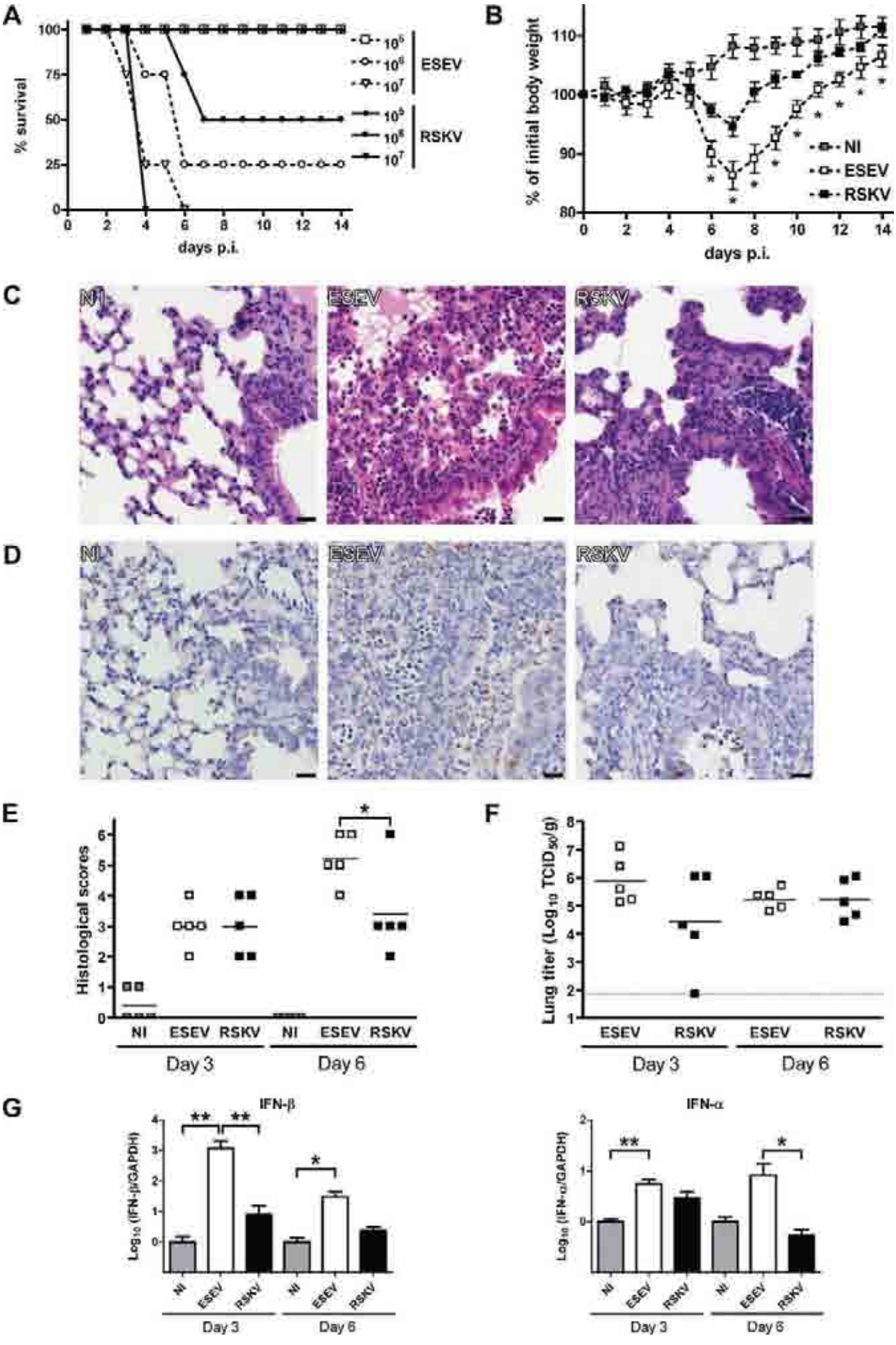
A
% survival
days p.i.
ESEV
RSKV
B
% of initial body weight
days p.i.
NI
ESEV
RSKV
C
NI
ESEV
RSKV
D
NI
ESEV
RSKV
E
Histological scores
NI ESEV RSKV NI ESEV RSKV
Day 3
Day 6
F
Lung titer (Log10 TCID50/g)
ESEV RSKV ESEV RSKV
Day 3
Day 6
G
IFN-β
Log10 (IFN-β/GAPDH)
IFN-α
Log10 (IFN-α/GAPDH)
NI ESEV RSKV NI ESEV RSKV
Day 3
Day 6

TABLE 2. Amino acid sequences of the C-terminal domain of NS1[a]

Animal	Virus inoculated	No. of clones sequenced/ total no. of animals
Mouse		
1	ESEV	10/10 ESEV
2	ESEV	12/12 ESEV
3	ESEV	13/13 ESEV
4	RSKV	11/11 RSKV
Duck		
1	RSKV	11/11 RSKV
2	RSKV	5/5 RSKV
3	RSKV	4/4 RSKV
4	ESEV	7/7 ESEV

[a] The amino acid sequence of the C-terminal domain of NS1 was determined as described in Materials and Methods. The number of clones sequenced for each animal is indicated. Virus was isolated from lungs of mice at day 6 p.i. and from cloacal swabs from ducks at day 14 p.i.

DISCUSSION

By comparing the virulences of recombinant LPAI H7N1 viruses in mice and ducks, we identified that the C-terminal domain of NS1 functions as a species-specific virulence domain. We show here for the first time that the C-terminal RSKV domain of NS1 increases virus replication in duck cells *in vitro* and *in vivo* as well as in human cells *in vitro*. In contrast, the C-terminal ESEV domain increases virulence in mice, confirming results previously obtained with the human influenza virus A/WSN/33 strain (24). Moreover, we show for the first time that the increased virulence is associated with an increase in levels of type I IFN production in lungs of ESEV-infected mice.

The E227R mutation in NS1 inevitably introduces an S70G mutation into NEP. Although we cannot completely rule out an effect of an NEP mutation, this possibility seems unlikely, as the NEPS70 and the NEPG70 viruses, which differ only by the S70G mutation in NEP, had indistinguishable phenotypes in human, mouse, and duck cells. This result strongly suggests that the differences observed between the ESEV and RSKV viruses can be attributed to amino acid changes in NS1.

Jackson et al. found previously that the C-terminal KSEV and EPEV domains of NS1 also enhanced virulence in mice similarly to the ESEV domain (24). NS1 proteins with C-terminal ESEV, KSEV, and EPEV domains were shown to bind to PDZ domains containing cellular proteins (32, 47). The increased virulence of these influenza viruses in mice has been linked to their ability to interact with PDZ domains of cellular proteins, although the identity of these cellular proteins and the cellular pathways affected remain unknown. However, our findings show that the role of PDZ-containing cellular proteins in modulating influenza virus virulence may depend on the host species. Indeed, RSKV, which lacks a PDZ binding domain, replicated to higher titers than ESEV in human and duck cells, suggesting that the ability of NS1 to interact with PDZ-containing proteins does not contribute to virulence in these host species.

Our results show that ESEV induced higher levels of type I IFN than RSKV in mouse cells but that ESEV was less sensitive to type I IFN pretreatment. This property could enable ESEV to reach higher titers than RSKV during multiple-cycle growth in mouse cells, even though it replicates to lower titers during single-cycle growth and induces higher levels of type I IFN than RSKV. Insensitivity to IFN pretreatment was previously described for certain strains of H5N1 viruses and was correlated with the presence of a glutamic acid at position 92 of NS1 (39). Variation in the sensitivity to IFN pretreatment has also been attributed to mutations of amino acids 38 and 41 of NS1, which are part of the RNA binding domain of NS1 (28). However, ESEV and RSKV both have an aspartic acid at position 92 of NS1 and do not differ from each other at amino acids 38 and 41. Interestingly, the lack of a correlation between IFN production and viral growth in mammalian cells *in vitro* was previously observed for certain strains of influenza virus (16, 17). In addition, viral genes other than NS1 have been shown to modulate sensitivity to type I IFN-induced effectors (4, 46). Further studies are needed to understand how certain strains of influenza virus are able to grow in mammalian cells even though they induce large amounts of type I IFN. ESEV also induced high levels of type I IFN in the lungs, and we found that the higher virulence of ESEV in mice *in vivo* correlated with type I IFN levels rather than with viral load. The strong type I IFN production and the massive amounts of neutrophil and mononuclear cell infiltrates in the lungs of ESEV-infected mice are reminiscent of the excessive lung inflammation observed with highly pathogenic avian influenza virus H5N1 or with the reconstructed H1N1 strain from 1918 (1, 27, 33). In future studies, it would be interesting to evaluate the phenotype of the ESEV and RSKV viruses in mice carrying functional *Mx1* alleles. *Mx1* is an interferon-stimulated gene encoding a protein that is a potent inhibitor of influenza viruses in mice (14, 37, 48). We cannot exclude that ESEV,

FIG. 8. Replication and pathogenesis in mice. (A) Survival of mice inoculated with the indicated amounts of ESEV or RSKV (four mice per group). (B) Percent change in weight following inoculation with 10^5 PFU of ESEV or RSKV. *, $P < 0.05$ by unpaired *t* test between ESEV- and RSKV-infected mice (five mice per group). (C) Mouse lung tissue collected at day 6 p.i. from mice inoculated with 10^5 PFU ESEV or RSKV (formalin fixation, 3-μm sections, H&E staining, and ×20 magnification) (bar, 20 μm). NI, no lesion; ESEV, severe bronchioloalveolitis; RSKV, moderate bronchioloalveolitis. (D) Immunohistochemical anti-NP staining of 3-μm lung sections from the animals presented in C (hematoxylin counterstaining and ×20 magnification) (bar, 20 μm). Shown is the staining of bronchiolar epithelial cells and a few macrophages in ESEV- and RSKV-infected mice. (E) Histological scoring of H&E-stained lung sections (squares, individual score; bars, mean score). (F) Viral load in lungs of mice infected with 10^5 PFU of ESEV or RSKV. Lungs were collected at days 3 and 6 p.i. and titrated with MDCK cells (squares, individual titer; bars, mean titer; dotted line, detection limit [here $10^{1.85}$ $TCID_{50}$/g]). (G) RT-qPCR analysis of type I IFN produced at days 3 and 6 p.i. in lungs of mice infected with 10^5 PFU of ESEV or RSKV. IFN-β and IFN-α levels are normalized to GAPDH levels, and results are expressed as fold induction compared with noninfected animals. Results are expressed as means ± SEM of data from five mice per group. *, $P < 0.05$; **, $P < 0.01$ (by unpaired *t* test).

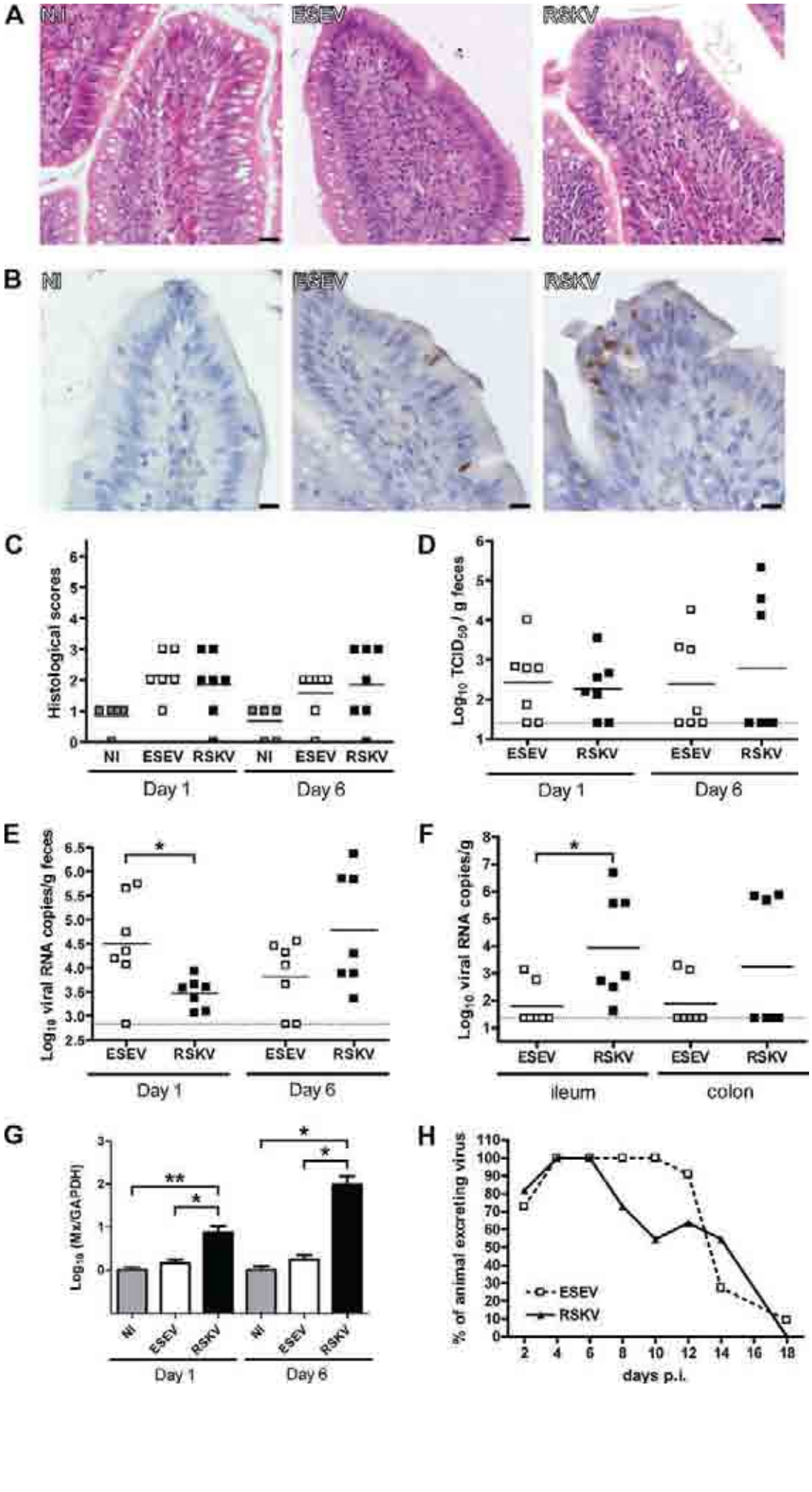
A
NI
ESEV
RSKV
B
NI
ESEV
RSKV
C
Histological scores
NI
ESEV
RSKV
NI
ESEV
RSKV
Day 1
Day 6
D
Log10 TCID50 / g feces
ESEV
RSKV
ESEV
RSKV
Day 1
Day 6
E
Log10 viral RNA copies/g feces
*
ESEV
RSKV
ESEV
RSKV
Day 1
Day 6
F
Log10 viral RNA copies/g
*
ESEV
RSKV
ESEV
RSKV
ileum
colon
G
Log10 (Mx/GAPDH)
**
*
*
*
NI
ESEV
RSKV
NI
ESEV
RSKV
Day 1
Day 6
H
% of animal excreting virus
ESEV
RSKV
days p.i.

which is a strong type I IFN inducer, could be partially attenuated in *Mx1*$^{+/+}$ mice compared to *Mx1*-deficient mice.

RSKV replicates to higher titers than ESEV in human and duck cells, and this increase in viral replication is associated with an increase in levels of type I IFN production *in vitro*. RSKV also replicates to higher levels in ducks *in vivo* and induces higher levels of *Mx* transcripts, likely reflecting an increase in levels of type I IFN production *in vivo*. In contrast to mouse cells, ESEV and RSKV did not differ in their sensitivities to type I IFN pretreatment in human and duck cells. Altogether, these results indicate that NS1 with a C-terminal RSKV domain does not increase virus replication by inhibiting type I IFN synthesis or type I IFN-induced effectors more efficiently than NS1 with a C-terminal ESEV domain. In contrast, our results show that RSKV reached significantly higher titers than ESEV during single-cycle growth, suggesting that NS1 with a human C-terminal RSKV domain increases the intrinsic virus growth speed. NS1 was previously shown to modulate viral polymerase activity (9, 29). Thus, NS1 with a C-terminal RSKV domain could increase viral replication in human and duck cells by regulating viral polymerase activity. However, further studies are needed to test this hypothesis.

ESEV was excreted at higher levels in duck feces at day 1 p.i., but intriguingly, no viral RNA could be detected in the ileal and colonic mucosae of these animals. The higher level of fecal excretion observed for ESEV-infected ducks at day 1 p.i. could therefore be due to remains of the viral inoculum administered orally or due to viral replication upstream in the intestine. However, the ileum and the colon have been repeatedly shown to be the major sites of LPAI virus replication in duck intestine (26, 51; our unpublished observations). At day 6 p.i., we also found that five of the seven ESEV-infected ducks excreted viral RNA in the feces, whereas only two of the seven ESEV-inoculated ducks had detectable amounts of viral RNA in either the ileal or colonic mucosae (Fig. 9E and F). We found that differentiated intestinal epithelial cells were the major site of ESEV and RSKV replication, as shown immunohistochemically with anti-NP staining (Fig. 9B). We therefore hypothesize that the higher viral load found in the feces than in the intestinal mucosa could result from the rapid desquamation of infected differentiated intestinal epithelial cells. Other authors previously identified undifferentiated epithelial cells in the intestinal crypts as the major site of LPAI virus replication in ducks (23, 26). However, using virus histochemistry, Munster et al. showed that an avian H7N7 virus was able to attach to differentiated duck colonic epithelial cells, indicating that these cells express viral receptors (30). Thus, the precise histological localization of LPAI virus replication in the duck intestine is likely to be influenced by the viral strain or by host-dependent determinants.

Large-scale sequence analyses have shown that NS1 is under strong selection pressure and evolves at a rate similar to those of HA and NA (3, 5, 32). The existence of a typical human C-terminal RSKV domain in NS1 and a typical avian C-terminal ESEV domain in NS1 could be an illustration of this phenomenon. As they are selected during evolution, these C-terminal domains are likely to confer a phenotypic advantage, for example, through interactions with specific binding partners in their respective natural hosts. Our results show that, indeed, the C-terminal RSKV domain increases virus replication in human cells. However, unexpectedly, we show that the typical human RSKV domain also increases virus replication in ducks. Ducks are the natural reservoirs of avian influenza viruses and are therefore most likely a species in which the typical avian C-terminal ESEV domain of NS1 is selected during virus evolution. If the ESEV domain decreases virus replication in ducks compared to RSKV, why is the ESEV domain selected during virus evolution in ducks? One possible explanation is that a pathogen that is less virulent can persist longer in its host, for example, by inducing a weaker immune response. Our data are in accordance with this hypothesis, as ESEV induced fewer type I IFN-stimulated gene transcripts in ducks than did the human-like RSKV. In addition, by analyzing cloacal swabs from infected ducks, we show that ESEV tended to be excreted for a longer period than RSKV. Being excreted longer possibly means that the virus can contaminate more individuals. Valuable information would certainly be obtained by evaluating the transmissibility of the ESEV and RSKV viruses in ducks (35, 43, 49) and in a suitable mammalian model, such as the ferret (18, 41). Finally, viral sequence analysis after rounds of natural interhost transmission could enable the evaluation of the mutation rate of the sequence encoding the C-terminal domain of NS1.

The majority of influenza viruses have a 230-amino-acid-long NS1 protein with a consensus ESEV C-terminal domain found in 78% of avian influenza virus isolates or a consensus human RSVK domain found in 85% of the typical human influenza virus isolates (32). However, NS1 proteins of various lengths also exist, and C-terminally truncated NS1 proteins have been isolated, mainly from birds and swine (6, 7). The

FIG. 9. Replication and pathogenesis in ducks. Two-week-old Pekin ducks were inoculated with 10^7 PFU ESEV or RSKV. (A) Ileum collected at day 6 p.i. (formalin fixation, 3-μm sections, H&E staining, and ×20 magnification) (bar, 20 μm). NI, no lesion; ESEV, mild enteritis; RSKV, mild enteritis. (B) Immunohistochemical anti-NP staining of 3-μm ileum sections from the animals presented in A (hematoxylin counterstaining and ×40 magnification) (bar, 40 μm). Shown is staining of enterocytes at the tip of the villi in ESEV- and RSKV-infected ducks. (C) Histological scoring of H&E-stained ileum sections (squares, individual score; bars, mean score). (D) The viral load in the feces of animals autopsied at days 1 and 6 p.i. was titrated with MDCK cells (squares, individual titer; bars, mean titer; dotted line, detection limit [here $10^{1.4}$ $TCID_{50}$/g]). (E) Viral RNA level in the feces of animals autopsied at days 1 and 6 p.i. Viral RNA levels were determined by one-step RT-qPCR (squares, individual level; bars, mean level; dotted line, detection limit [here $10^{2.8}$ viral RNA copies/g]). (F) Viral RNA level in the ileal and colonic mucosae at day 6 p.i. Viral RNA levels from scraped mucosae were determined by one-step RT-qPCR (squares, individual level; bars, mean level; dotted line, detection limit [here $10^{1.3}$ viral RNA copies/g]). (G) RT-qPCR analysis of *Mx* expression at days 1 and 6 p.i. in the ileum of ducks. *Mx* levels are normalized to GAPDH levels, and results are expressed as fold induction compared with noninfected animals. Results are expressed as means ± SEM of data from six noninfected animals and seven infected animals in each group. (H) Duration of viral shedding in droppings. Cloacal swabs collected following infection were analyzed by one-step RT-qPCR to detect viral nucleic acid. Results are expressed as percent positive animals over time. *, $P < 0.05$; **, $P < 0.01$ (by unpaired *t* test).

"classical swine" H1N1 virus has been circulating in pigs since the mid-1960s, with a 219-amino-acid-long NS1 protein. This 219-amino-acid-long NS1 protein is now present in the novel 2009 H1N1 strain circulating in the human population worldwide (10). A recent study has shown that increasing the length of the 2009 H1N1 NS1 protein to 230 amino acids does not increase virus replication in human and pig cells (13). Altogether, these results suggest that the contribution of the C-terminal domain of NS1 to virulence or viral fitness could also depend on the viral strain. The presence of other virulence determinants in NS1 or in other viral proteins may compensate for the lack of a C-terminal domain in NS1. Therefore, further studies are required to study how the genetic background of a virus may determine to which extent the C-terminal domain of NS1 modulates virulence and viral fitness.

ACKNOWLEDGMENTS

We thank I. Capua for the kind gift of viruses, D. Marc and G. Whittaker for the kind gift of antibodies, and R. Webster, P. Staeheli, and U. Schultz for the kind gift of plasmids. We thank D. Gonzalez-Dunia for critical reading of the manuscript and insightful comments.

This work was supported by grants from INRA and Comité Interprofessionnel des Palmipèdes à Foie Gras. S.M.S. is the recipient of a doctoral fellowship from the French Ministry of Research.

REFERENCES

1. **Baskin, C. R., H. Bielefeldt-Ohmann, T. M. Tumpey, P. J. Sabourin, J. P. Long, A. Garcia-Sastre, A. E. Tolnay, R. Albrecht, J. A. Pyles, P. H. Olson, L. D. Aicher, E. R. Rosenzweig, K. Murali-Krishna, E. A. Clark, M. S. Kotur, J. L. Fornek, S. Proll, R. E. Palermo, C. L. Sabourin, and M. G. Katze.** 2009. Early and sustained innate immune response defines pathology and death in nonhuman primates infected by highly pathogenic influenza virus. Proc. Natl. Acad. Sci. U. S. A. **106:**3455–3460.
2. **Chen, G. W., S. C. Chang, C. K. Mok, Y. L. Lo, Y. N. Kung, J. H. Huang, Y. H. Shih, J. Y. Wang, C. Chiang, C. J. Chen, and S. R. Shih.** 2006. Genomic signatures of human versus avian influenza A viruses. Emerg. Infect. Dis. **12:**1353–1360.
3. **Chen, R., and E. C. Holmes.** 2006. Avian influenza virus exhibits rapid evolutionary dynamics. Mol. Biol. Evol. **23:**2336–2341.
4. **Dittmann, J., S. Stertz, D. Grimm, J. Steel, A. Garcia-Sastre, O. Haller, and G. Kochs.** 2008. Influenza A virus strains differ in sensitivity to the antiviral action of Mx-GTPase. J. Virol. **82:**3624–3631.
5. **Dugan, V. G., R. Chen, D. J. Spiro, N. Sengamalay, J. Zaborsky, E. Ghedin, J. Nolting, D. E. Swayne, J. A. Runstadler, G. M. Happ, D. A. Senne, R. Wang, R. D. Slemons, E. C. Holmes, and J. K. Taubenberger.** 2008. The evolutionary genetics and emergence of avian influenza viruses in wild birds. PLoS Pathog. **4:**e1000076.
6. **Dundon, W., and I. Capua.** 2009. A closer look at the NS1 of influenza virus. Viruses **1:**1057–1072.
7. **Dundon, W. G., A. Milani, G. Cattoli, and I. Capua.** 2006. Progressive truncation of the non-structural 1 gene of H7N1 avian influenza viruses following extensive circulation in poultry. Virus Res. **119:**171–176.
8. **Dunn, G. P., A. T. Bruce, K. C. Sheehan, V. Shankaran, R. Uppaluri, J. D. Bui, M. S. Diamond, C. M. Koebel, C. Arthur, J. M. White, and R. D. Schreiber.** 2005. A critical function for type I interferons in cancer immunoediting. Nat. Immunol. **6:**722–729.
9. **Falcón, A. M., R. M. Marion, T. Zurcher, P. Gomez, A. Portela, A. Nieto, and J. Ortin.** 2004. Defective RNA replication and late gene expression in temperature-sensitive influenza viruses expressing deleted forms of the NS1 protein. J. Virol. **78:**3880–3888.
10. **Garten, R. J., C. T. Davis, C. A. Russell, B. Shu, S. Lindstrom, A. Balish, W. M. Sessions, X. Xu, E. Skepner, V. Deyde, M. Okomo-Adhiambo, L. Gubareva, J. Barnes, C. B. Smith, S. L. Emery, M. J. Hillman, P. Rivailler, J. Smagala, M. de Graaf, D. F. Burke, R. A. Fouchier, C. Pappas, C. M. Alpuche-Aranda, H. Lopez-Gatell, H. Olivera, I. Lopez, C. A. Myers, D. Faix, P. J. Blair, C. Yu, K. M. Keene, P. D. Dotson, Jr., D. Boxrud, A. R. Sambol, S. H. Abid, K. St. George, T. Bannerman, A. L. Moore, D. J. Stringer, P. Blevins, G. J. Demmler-Harrison, M. Ginsberg, P. Kriner, S. Waterman, S. Smole, H. F. Guevara, E. A. Belongia, P. A. Clark, S. T. Beatrice, R. Donis, J. Katz, L. Finelli, C. B. Bridges, M. Shaw, D. B. Jernigan, T. M. Uyeki, D. J. Smith, A. I. Klimov, and N. J. Cox.** 2009. Antigenic and genetic characteristics of swine-origin 2009 A (H1N1) influenza viruses circulating in humans. Science **325:**197–201.
11. **Grimm, D., P. Staeheli, M. Hufbauer, I. Koerner, L. Martinez-Sobrido, A. Solorzano, A. Garcia-Sastre, O. Haller, and G. Kochs.** 2007. Replication fitness determines high virulence of influenza A virus in mice carrying functional Mx1 resistance gene. Proc. Natl. Acad. Sci. U. S. A. **104:**6806–6811.
12. **Hale, B. G., R. E. Randall, J. Ortin, and D. Jackson.** 2008. The multifunctional NS1 protein of influenza A viruses. J. Gen. Virol. **89:**2359–2376.
13. **Hale, B. G., J. Steel, B. Manicassamy, R. A. Medina, J. Ye, D. Hickman, A. C. Lowen, D. R. Perez, and A. Garcia-Sastre.** Mutations in the NS1 C-terminal tail do not enhance replication or virulence of the 2009 pandemic H1N1 influenza A virus. J. Gen. Virol., in press.
14. **Haller, O., H. Arnheiter, I. Gresser, and J. Lindenmann.** 1981. Virus-specific interferon action. Protection of newborn Mx carriers against lethal infection with influenza virus. J. Exp. Med. **154:**199–203.
15. **Hatta, M., Y. Hatta, J. H. Kim, S. Watanabe, K. Shinya, T. Nguyen, P. S. Lien, Q. M. Le, and Y. Kawaoka.** 2007. Growth of H5N1 influenza A viruses in the upper respiratory tracts of mice. PLoS Pathog. **3:**1374–1379.
16. **Hayman, A., S. Comely, A. Lackenby, L. C. Hartgroves, S. Goodbourn, J. W. McCauley, and W. S. Barclay.** 2007. NS1 proteins of avian influenza A viruses can act as antagonists of the human alpha/beta interferon response. J. Virol. **81:**2318–2327.
17. **Hayman, A., S. Comely, A. Lackenby, S. Murphy, J. McCauley, S. Goodbourn, and W. Barclay.** 2006. Variation in the ability of human influenza A viruses to induce and inhibit the IFN-beta pathway. Virology **347:**52–64.
18. **Herlocher, M. L., S. Elias, R. Truscon, S. Harrison, D. Mindell, C. Simon, and A. S. Monto.** 2001. Ferrets as a transmission model for influenza: sequence changes in HA1 of type A (H3N2) virus. J. Infect. Dis. **184:**542–546.
19. **Hoffmann, E., G. Neumann, Y. Kawaoka, G. Hobom, and R. G. Webster.** 2000. A DNA transfection system for generation of influenza A virus from eight plasmids. Proc. Natl. Acad. Sci. U. S. A. **97:**6108–6113.
20. **Hoffmann, E., J. Stech, Y. Guan, R. G. Webster, and D. R. Perez.** 2001. Universal primer set for the full-length amplification of all influenza A viruses. Arch. Virol. **146:**2275–2289.
21. **Holzinger, D., C. Jorns, S. Stertz, S. Boisson-Dupuis, R. Thimme, M. Weidmann, J. L. Casanova, O. Haller, and G. Kochs.** 2007. Induction of MxA gene expression by influenza A virus requires type I or type III interferon signaling. J. Virol. **81:**7776–7785.
22. **Horimoto, T., and Y. Kawaoka.** 2001. Pandemic threat posed by avian influenza A viruses. Clin. Microbiol. Rev. **14:**129–149.
23. **Ito, T., Y. Suzuki, T. Suzuki, A. Takada, T. Horimoto, K. Wells, H. Kida, K. Otsuki, M. Kiso, H. Ishida, and Y. Kawaoka.** 2000. Recognition of N-glycolylneuraminic acid linked to galactose by the alpha2,3 linkage is associated with intestinal replication of influenza A virus in ducks. J. Virol. **74:**9300–9305.
24. **Jackson, D., M. J. Hossain, D. Hickman, D. R. Perez, and R. A. Lamb.** 2008. A new influenza virus virulence determinant: the NS1 protein four C-terminal residues modulate pathogenicity. Proc. Natl. Acad. Sci. U. S. A. **105:**4381–4386.
25. **Kawaoka, Y., O. T. Gorman, T. Ito, K. Wells, R. O. Donis, M. R. Castrucci, I. Donatelli, and R. G. Webster.** 1998. Influence of host species on the evolution of the nonstructural (NS) gene of influenza A viruses. Virus Res. **55:**143–156.
26. **Kida, H., R. Yanagawa, and Y. Matsuoka.** 1980. Duck influenza lacking evidence of disease signs and immune response. Infect. Immun. **30:**547–553.
27. **Kobasa, D., S. M. Jones, K. Shinya, J. C. Kash, J. Copps, H. Ebihara, Y. Hatta, J. H. Kim, P. Halfmann, M. Hatta, F. Feldmann, J. B. Alimonti, L. Fernando, Y. Li, M. G. Katze, H. Feldmann, and Y. Kawaoka.** 2007. Aberrant innate immune response in lethal infection of macaques with the 1918 influenza virus. Nature **445:**319–323.
28. **Min, J. Y., and R. M. Krug.** 2006. The primary function of RNA binding by the influenza A virus NS1 protein in infected cells: inhibiting the 2′-5′ oligo(A) synthetase/RNase L pathway. Proc. Natl. Acad. Sci. U. S. A. **103:**7100–7105.
29. **Min, J. Y., S. Li, G. C. Sen, and R. M. Krug.** 2007. A site on the influenza A virus NS1 protein mediates both inhibition of PKR activation and temporal regulation of viral RNA synthesis. Virology **363:**236–243.
30. **Munster, V. J., E. de Wit, D. van Riel, W. E. Beyer, G. F. Rimmelzwaan, A. D. Osterhaus, T. Kuiken, and R. A. Fouchier.** 2007. The molecular basis of the pathogenicity of the Dutch highly pathogenic human influenza A H7N7 viruses. J. Infect. Dis. **196:**258–265.
31. **Neumann, G., T. Noda, and Y. Kawaoka.** 2009. Emergence and pandemic potential of swine-origin H1N1 influenza virus. Nature **459:**931–939.
32. **Obenauer, J. C., J. Denson, P. K. Mehta, X. Su, S. Mukatira, D. B. Finkelstein, X. Xu, J. Wang, J. Ma, Y. Fan, K. M. Rakestraw, R. G. Webster, E. Hoffmann, S. Krauss, J. Zheng, Z. Zhang, and C. W. Naeve.** 2006. Large-scale sequence analysis of avian influenza isolates. Science **311:**1576–1580.
33. **Perrone, L. A., J. K. Plowden, A. Garcia-Sastre, J. M. Katz, and T. M. Tumpey.** 2008. H5N1 and 1918 pandemic influenza virus infection results in early and excessive infiltration of macrophages and neutrophils in the lungs of mice. PLoS Pathog. **4:**e1000115.
34. **Petri, T., and N. J. Dimmock.** 1981. Phosphorylation of influenza virus nucleoprotein in vivo. J. Gen. Virol. **57:**185–190.
35. **Pillai, S. P., D. L. Suarez, M. Pantin-Jackwood, and C. W. Lee.** 2008.

Pathogenicity and transmission studies of H5N2 parrot avian influenza virus of Mexican lineage in different poultry species. Vet. Microbiol. **129:**48–57.
36. **Rameix-Welti, M. A., A. Tomoiu, E. Dos Santos Afonso, S. van der Werf, and N. Naffakh.** 2009. Avian influenza A virus polymerase association with nucleoprotein, but not polymerase assembly, is impaired in human cells during the course of infection. J. Virol. **83:**1320–1331.
37. **Salomon, R., P. Staeheli, G. Kochs, H. L. Yen, J. Franks, J. E. Rehg, R. G. Webster, and E. Hoffmann.** 2007. Mx1 gene protects mice against the highly lethal human H5N1 influenza virus. Cell Cycle **6:**2417–2421.
38. **Schumacher, B., D. Bernasconi, U. Schultz, and P. Staeheli.** 1994. The chicken Mx promoter contains an ISRE motif and confers interferon inducibility to a reporter gene in chick and monkey cells. Virology **203:**144–148.
39. **Seo, S. H., E. Hoffmann, and R. G. Webster.** 2002. Lethal H5N1 influenza viruses escape host anti-viral cytokine responses. Nat. Med. **8:**950–954.
40. **Sommereyns, C., S. Paul, P. Staeheli, and T. Michiels.** 2008. IFN-lambda (IFN-lambda) is expressed in a tissue-dependent fashion and primarily acts on epithelial cells in vivo. PLoS Pathog. **4:**e1000017.
41. **Sorrell, E. M., H. Wan, Y. Araya, H. Song, and D. R. Perez.** 2009. Minimal molecular constraints for respiratory droplet transmission of an avian-human H9N2 influenza A virus. Proc. Natl. Acad. Sci. U. S. A. **106:**7565–7570.
42. **Soubies, S., C. Volmer, J. Guérin, and R. Volmer.** 2010. Truncation of the NS1 protein converts a low pathogenic avian influenza virus into a strong interferon inducer in duck cells. Avian Dis. **54:**527–531.
43. **Spackman, E., D. E. Swayne, D. L. Suarez, D. A. Senne, J. C. Pedersen, M. L. Killian, J. Pasick, K. Handel, S. P. Pillai, C. W. Lee, D. Stallknecht, R. Slemons, H. S. Ip, and T. Deliberto.** 2007. Characterization of low-pathogenicity H5N1 avian influenza viruses from North America. J. Virol. **81:**11612–11619.
44. **Steel, J., A. C. Lowen, S. Mubareka, and P. Palese.** 2009. Transmission of influenza virus in a mammalian host is increased by PB2 amino acids 627K or 627E/701N. PLoS Pathog. **5:**e1000252.
45. **Subbarao, E. K., W. London, and B. R. Murphy.** 1993. A single amino acid in the PB2 gene of influenza A virus is a determinant of host range. J. Virol. **67:**1761–1764.
46. **Szretter, K. J., S. Gangappa, J. A. Belser, H. Zeng, H. Chen, Y. Matsuoka, S. Sambhara, D. E. Swayne, T. M. Tumpey, and J. M. Katz.** 2009. Early control of H5N1 influenza virus replication by the type I interferon response in mice. J. Virol. **83:**5825–5834.
47. **Tonikian, R., Y. Zhang, S. L. Sazinsky, B. Currell, J. H. Yeh, B. Reva, H. A. Held, B. A. Appleton, M. Evangelista, Y. Wu, X. Xin, A. C. Chan, S. Seshagiri, L. A. Lasky, C. Sander, C. Boone, G. D. Bader, and S. S. Sidhu.** 2008. A specificity map for the PDZ domain family. PLoS Biol. **6:**e239.
48. **Tumpey, T. M., K. J. Szretter, N. Van Hoeven, J. M. Katz, G. Kochs, O. Haller, A. Garcia-Sastre, and P. Staeheli.** 2007. The Mx1 gene protects mice against the pandemic 1918 and highly lethal human H5N1 influenza viruses. J. Virol. **81:**10818–10821.
49. **van der Goot, J. A., M. van Boven, A. Stegeman, S. G. van de Water, M. C. de Jong, and G. Koch.** 2008. Transmission of highly pathogenic avian influenza H5N1 virus in Pekin ducks is significantly reduced by a genetically distant H5N2 vaccine. Virology **382:**91–97.
50. **Volmer, R., C. Monnet, and D. Gonzalez-Dunia.** 2006. Borna disease virus blocks potentiation of presynaptic activity through inhibition of protein kinase C signaling. PLoS Pathog. **2:**e19.
51. **Webster, R. G., M. Yakhno, V. S. Hinshaw, W. J. Bean, and K. G. Murti.** 1978. Intestinal influenza: replication and characterization of influenza viruses in ducks. Virology **84:**268–278.
52. **Yamada, S., Y. Suzuki, T. Suzuki, M. Q. Le, C. A. Nidom, Y. Sakai-Tagawa, Y. Muramoto, M. Ito, M. Kiso, T. Horimoto, K. Shinya, T. Sawada, M. Kiso, T. Usui, T. Murata, Y. Lin, A. Hay, L. F. Haire, D. J. Stevens, R. J. Russell, S. J. Gamblin, J. J. Skehel, and Y. Kawaoka.** 2006. Haemagglutinin mutations responsible for the binding of H5N1 influenza A viruses to human-type receptors. Nature **444:**378–382.